Magnetically Tunable Nonreciprocal Band-Pass Filters Using Ferrimagnetic Resonators*

C. N. PATEL†, MEMBER, IRE

Summary—Possibilities of a small-bandwidth, small-insertion loss, magnetically tunable band-pass filters with nonreciprocal characteristics have been studied. The unloaded $Q(Q_u)$ for a ferrimagnetic sample has been derived, considering the fundamental definition of Q for a resonator. Theoretical analysis is given for coupling due to ferrimagnetic resonance, between two RF transmission circuits when the RF magnetic fields due to the two circuits are circularly polarized or, in general, elliptically polarized. The analysis gives the open-circuit impedance parameters for the equivalent circuit representing the ferrimagnetic coupling mechanism, from which the external-loading Q's (Q_{e_1} and Q_{e_2}) are obtained. This analysis, applied to the case of the waveguides, shows that the behavior of the Q_e vs frequency characteristic depends upon the ellipticity of the RF magnetic field, and hence, upon the location of the off-axis position of the ferrimagnetic resonator. Also, the nonreciprocity depends upon the ellipticity of the RF magnetic field—the nonreciprocal behavior being optimum when the RF magnetic field is circularly polarized. Thus, again, for the case of waveguide circuits, the off-axis position determines the reverse-coupling-vs-frequency characteristic. The measurements on the experimental filters, tunable from 8.2 to 12.4 kMc, verify the results obtained from the theory. The forward and the reverse directions of the operation of these filters can be interchanged by reversing the dc magnetic field. Power limiting with these filters is briefly described.

Introduction

THE SIMPLEST class of band-pass filters is the single-resonance transmission filter, which usually consists of a tunable resonator and input and output coupling loops. With the resonator is associated an unloaded $Q(Q_u)$ and with the coupling loops are associated the external or the loading Q's (Q_{e_1} and Q_{e_2}). It is the relative values of the Q_u and the Q_e that determine the minimum insertion loss within the pass band of the filter. To have a small insertion loss, the ratio of Q_u to the Q_e should be as high as possible. Hence, with a given bandwidth and the requirement that the insertion loss be as small as possible, the only choice is that of obtaining as high a Q_u as possible. At microwave frequencies, the resonators usually consist of quarter- or half-wavelength coaxial lines, cavities, etc., which are rather difficult to tune as they are tuned mechanically. Another mechanically tunable resonator for microwave frequencies is the traveling-wave ring resonator.[1]

The use of YIG spheres as high-Q microwave resonators was first reported by DeGrasse,[2] who used a tuned stripline structure to couple energy in and out of the resonator. However, it has been recognized since then that the mechanically tuned circuit, which robs the device of its magnetically tunable advantages, is indeed not necessary. Carter[3,4] has reported microwave magnetically tunable filters using broad-band coupling structures. Kotzebue[5] has reported a very lightweight magnetically tunable filter at S-band frequencies which certainly indicates that the requirements of dc magnetic field are not a serious problem as far as weight is concerned. But all these filters use linearly polarized RF magnetic fields of the coupling circuits, and are reciprocal. In order to take full advantage of all the characteristics of a ferrimagnetic resonator as far as nonreciprocity is concerned, one will have to use elliptically (in particular, circularly) polarized RF magnetic fields. This paper describes the analysis and experiments of filters that use elliptically polarized RF magnetic fields, for coupling energy into and out of the YIG resonator.

This paper can be roughly divided into two parts:

1) Theoretical analysis regarding the resonator and the coupling mechanism.
2) Experimental results on the various filters built to check the theory.

The unloaded $Q(Q_u)$ for a ferrimagnetic resonator of general shape has been derived using the basic definition of Q_u for a resonator. The results have been simplified for the case of an ellipsoid of revolution about the dc magnetic field, and for a spherical sample. The results

* Received by the PGMTT, May 29, 1961; revised manuscript received, August 11, 1961. The research reported herein was jointly supported by the U. S. Army Signal Corps, the U. S. Air Force and the U. S. Navy under the ONR Contract Nonr 225(24), NR 373 360 and is taken in large from the dissertation submitted by the author to the Department of Electrical Engineering of Stanford University, Calif., in partial fulfillment of the requirements for the degree of Ph.D. This paper was presented at WESCON, San Francisco, Calif., August 22–25, 1961.

† Bell Telephone Laboratory, Murray Hill, N. J. Formerly, Electronics Research Laboratory, Stanford University, Stanford, Calif.

[1] F. J. Tischer, "Resonant properties of nonreciprocal ring circuits," IRE TRANS. ON MICROWAVE THEORY AND TECHNIQUES, vol. MTT-6, pp. 66–72; January, 1958.

[2] R. W. DeGrasse, "Low loss gyromagnetic coupling through single crystal garnets," *J. Appl. Phys.*, vol. 30, pp. 155s–156s; April, 1959.

[3] P. S. Carter, Jr., "Design Criteria for Microwave Filters and Coupling Structures," Stanford Res. Inst., Menlo Park, Calif., Tech. Rept. No. 8, SRI Project No. 2326, Contract DA-36-039 SC-74862; September, 1959.

[4] P. S. Carter, Jr., "Unloaded Q of single crystal yttrium iron garnet resonator as function of frequency," IRE TRANS. ON MICROWAVE THEORY AND TECHNIQUES, vol. MTT-8, pp. 570–571; September, 1960.

[5] K. L. Kotzebue, "Broadband electronically tuned microwave filters," WESCON CONVENTION RECORD, pt. 1, vol. 4, pp. 21–27; 1960.

are independent of type of damping. The susceptibility tensor components for a ferrimagnetic material relating the external magnetic fields to the magnetization in the sample have been derived using Landau-Lifshitz and Bloch-Bloembergen formulation of equations of motion. The results show that for a spherical sample the *L-L* formulation gives Q_u for the sample, as seen from the resonance behavior of external susceptibility which agrees with the above. On the other hand, the *B-B* formulation gives a slightly different result. In this paper the *L-L* damping results are used and are believed to be more appropriate.

The coupling, due to the ferrimagnetic sample, from one structure to the other when the RF magnetic fields are elliptically polarized, is obtained by getting open-circuit impedance parameters for the YIG coupling equivalent circuit, and then from that deducing the external loading Q's from filter-circuit theory.[6,7] The general results have been applied to the case of a waveguide circuit. Using the filter structure shown in Fig. 1,

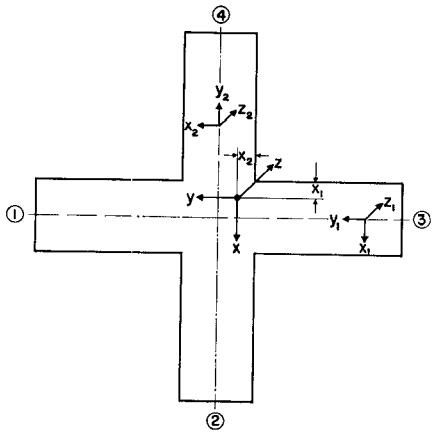

Fig. 1—Sketch of the structure analyzed to obtain the coupling parameters showing the coordinate axis and the port nomenclature. The coordinate axes at the YIG sphere are x, y, z.

the insertion-loss behavior between various ports is described in the form of a scattering matrix; the phase information in scattering-matrix elements has been left out as it is unimportant in considering the insertion loss. Here the nonreciprocal nature of the coupling becomes very evident.

The second part of the paper describes the various experimental structures on which measurements were carried out. Only the single-resonance filters were investigated, and the experimental results along with the theoretical results, showing a good agreement, are given. The power-limiting behavior of the filter is also reported, and the leakage-spike duration, amplitude and energy measurements are briefly described.

[6] C. H. Montgomery, R. H. Dicke and E. M. Purcell, "Principles of Microwave Circuits," McGraw-Hill Book Co., Inc., New York, N. Y., MIT Rad. Lab. Series, vol. 8, ch. 7; 1948.

[7] G. L. Ragan, "Microwave Transmission Circuits," McGraw-Hill Book Co., Inc., New York, N. Y., MIT Rad. Lab. Series, vol. 9, ch. 9 and 10; 1948.

Unloaded Q of the Ferrimagnetic Sample

Considering the ferrimagnetic sample to be a resonator, it is easy to find the Q_u associated with it from the basic results.

$$Q_u = \omega_0 \frac{\text{time average of RF energy stored in the sample}}{\text{power lost in the sample}}. \quad (1)$$

Assume a sample that is saturated in the z direction, due to the dc magnetic field and a small-signal RF magnetic field applied in a plane at right angles to the dc magnetic field. Consider only the case of circularly polarized RF magnetic fields at the frequency of resonance.

$$E = \text{time average of RF energy stored in the sample} \quad (2)$$

$$= \int_{\text{volume}} \left[\begin{array}{l}(\text{Energy density with the RF magnetic} \\ \text{field present}) - (\text{energy density with-} \\ \text{out the RF magnetic field})\end{array}\right] dv. \quad (3)$$

For the energy density, we have[8]

$$\text{energy density} = -H_0M + \frac{1}{2}\sum_j N_jM_j^2 + \text{anisotropy energy} + \text{exchange energy} + \text{strain energy} \quad (4)$$

where

H_0 = External dc magnetic field along z axis
M = Magnetization
N_j = Shape dependent demagnetization factor[9] along the three axes
M_j = Components of magnetization along the three axes.

Neglecting the anisotropy, exchange and strain energies (with single crystal samples) in the small signal case, and omitting lengthy mathematical derivation, we have

$$E = \int_{\text{volume}} \left[\frac{M_x^2 + M_y^2}{2}\left(\frac{H_0}{M_s} - N_z\right) + \tfrac{1}{2}(N_xM_x^2 + N_yM_y^2)\right] dv \quad (5)$$

where

M_s = Saturation magnetization of the sample.

The equation of motion of magnetization vector with Landau-Lifshitz[10] damping is given as

$$\frac{\partial M}{\partial t} = \gamma(M \times H) - \frac{\alpha\gamma}{|M|}[M \times (M \times H)] \quad (6)$$

[8] J. R. MacDonald, "Ferromagnetic resonance and internal field in ferromagnetic materials," *Proc. Phys. Soc.*, vol. A-64, pp. 968–983; November, 1950.

[9] C. Kittel, "On the theory of ferromagnetic resonance absorption," *Phys. Rev.*, vol. 73, pp. 155–161; January, 1948.

[10] L. Landau and L. Lifshitz, "On the theory of dispersion of magnetic permeability in ferromagnetic bodies," *Phys. Z., Sowjet.*, vol. 8, no. 2, pp. 153–169; 1935.

where

$$\frac{\alpha}{|M|}[M \times (M \times H)]$$

is the loss term and H is the internal magnetic field.

α = Landau-Lifshitz damping parameter

$$= \frac{\gamma \Delta H_0}{2\omega_0} \text{ at resonance}$$

$$\gamma = \mu_0 \gamma_0 = -\mu_0 \frac{ge}{2m} \tag{7}$$

where

g = Landé g factor
e = Electron change
m = Electron mass
μ_0 = Permeability of medium surrounding the sample
$\omega_0 = \gamma H_0$
ω = Signal frequency (z directed).

Under steady state, we have

$$P_l = \int_{\text{volume}} (\text{loss})\, dv \tag{8}$$

$$= \int_{\text{volume}} (M \times H) \cdot \omega dv. \tag{9}$$

Omitting lengthy mathematical derivation, for the small signal case, we have

$$P_l\Big|_{\text{resonance}} = \int_{\text{volume}} \left[\frac{\Delta H_0 \omega_0}{2\omega_m}(M_x^2 + M_y^2)\right] dv \tag{10}$$

where

$$\omega_m = \gamma M_s.$$

$$\therefore\ Q_u = \omega_0 \frac{\displaystyle\int_{\text{volume}} \left[\frac{M_x^2 + M_y^2}{2}\left(\frac{H_0}{M_s} - N_z\right) + \tfrac{1}{2}(N_x M_x^2 + N_y M_y^2)\right] dv}{\displaystyle\int_{\text{volume}} \left[\frac{\Delta H_0 \omega_0}{2\omega_m}(M_x^2 + M_y^2)\right] dv}. \tag{11}$$

For the case of uniform precession, M does not vary with location in the ferrimagnetic sample

$$\therefore\ Q_u = \omega_0 \frac{\left[\dfrac{M_x^2 + M_y^2}{2}\left(\dfrac{H_0}{M_s} - N_z\right) + \tfrac{1}{2}(N_x M_x^2 + N_y M_y^2)\right]}{\left[\dfrac{\Delta H_0 \omega_0}{2\omega_m}(M_x^2 + M_y^2)\right]}. \tag{12}$$

When the sample is an ellipsoid of revolution about the z-directed dc magnetic field, we have

$$Q_u = \omega_0 \frac{H_0 + (N_T - N_Z)M_s}{\Delta H_0} \tag{13}$$

where

N_T = Transverse demagnetization factor
N_Z = Demagnetization factor in z direction.

$$\therefore\ Q_u = \frac{\omega_r}{\gamma \Delta H_0}$$

where

$$\omega_r = \text{Resonance frequency.} \tag{14}$$

For a sphere $N_T = N_Z = \frac{1}{3}$ and we get

$$Q_u = \frac{\omega_0}{\gamma \Delta H_0} = \frac{H_0}{\Delta H_0}. \tag{15}$$

It should be noted that the results in (12)–(15) do not depend upon the type of damping used in calculating the P_l, and this can be verified readily by starting with, say, Bloch-Bloembergen formulation in (7). In general these results are valid as long as the sample is saturated. However, when $\omega \lessapprox \omega_m/3$ the spherical sample is no longer saturated and the above expressions cannot be correctly used. The above results are different from those reported by Carter[4] and give slightly higher numerical results, but as seen from the analysis, the results are independent of the kind of damping used, *i.e.*, either L-L or B-B and hence, are more appropriate.

The linewidth depends upon the orientation of the crystal axis with the dc magnetic field. The linewidth is smallest when the dc field is oriented in the direction of the hard axis (100), and it is largest when the magnetic field is along the easy axis (111), as reported by Callen and Pittelli,[11] and by LeCraw, *et al.*[12] Thus the

[11] H. Callen and E. Pittelli, "Anisotropic ferromagnetic resonance linewidth in ferrites," *Phys. Rev.*, vol. 119, pp. 1523–1537; September, 1960.

[12] P. C. LeCraw, E. G. Spencer and C. S. Porter, "Ferromagnetic resonance linewidth in YIG single crystals," *Phys. Rev.*, vol. 110, pp. 1311–1313; June, 1958.

Q_u will depend upon the orientation. It can be seen from (13) and (14) that the cylindrical geometry gives higher Q_u, especially at lower frequencies, at which the spherical sample is no longer saturated. The orientation problem described above makes the preparation of a cylindrical sample, which is very finely polished and also has the hard axis along the axis of the cylinder, very difficult, although this is possible in theory. Also it is seen that for a cylindrical geometry $\omega_r=\gamma(H_0+M_s/2)$ and therefore the sample cannot possibly resonate at frequencies lower than $\omega=\gamma M_s/2$, which is higher than $\omega_m/3$; hence, one would be better off using spherical samples rather than cylindrical. The other possibility is using a sample with lower M_s, but this results in loss of coupling which will be discussed in greater detail in the section on coupling.

External Tensor Susceptibility Components

With a ferrimagnetic sample of finite size and shape, the magnetic fields inside are not the same as external magnetic fields, due to demagnetizing fields.[9] The equations of motion of the magnetization vector, including the phenomenological damping mechanism, such as the Landau-Lifshitz,[10] Bloch-Bloembergen[13] or Callen's three-parameter formulation,[14] relate the magnetization vector to the internal magnetic fields. As the samples used in the experiments in general are of finite size and shape, it is necessary to obtain a tensor susceptibility relationship between the magnetization vector and the external magnetic fields. The tensor susceptibility components are derived for the case of Landau-Lifshitz and Bloch-Bloembergen damping cases to determine the suitability of the two cases. The same assumptions as those in the previous section are made.

Writing

$$\boldsymbol{M}=\chi_{\text{ext}}\cdot\boldsymbol{H}_{\text{ext}}=\begin{pmatrix}\chi_1 & -j\mathcal{K} & 0\\ j\mathcal{K} & \chi_2 & 0\\ 0 & 0 & 1\end{pmatrix}\cdot\boldsymbol{H}_{\text{ext}}. \tag{16}$$

The problem is to find the components of the tensor as a result of the small-signal assumption.

Assuming a steady-state solution of the type $e^{j\omega t}$, we will state the results, omitting lengthy mathematical derivations.

Bloch-Bloembergen Case

The external tensor susceptibility components in this case have been derived elsewhere[3] and only the final results for the case of a spherical sample will be given.

$$\chi_1=\chi_2=\frac{\omega_m\omega_0}{\omega_0^2-\omega^2+\dfrac{2j\omega}{\tau}\left(\dfrac{\omega_0}{\omega_0-\dfrac{\omega_m}{3}}\right)} \tag{17}$$

and

$$\mathcal{K}=\frac{\omega_m\omega}{\omega_0^2-\omega^2+\dfrac{2j\omega}{\tau}\left(\dfrac{\omega_0}{\omega_0-\dfrac{\omega_m}{3}}\right)}. \tag{18}$$

With $\tau=2/\gamma\Delta H_0$, the resonance behavior of the external susceptibility yields

$$Q_u\Big|_{\text{sphere, }B\text{-}B\text{ formulation}}=\frac{H_0}{\Delta H_0}\left(\frac{H_0-\dfrac{M_s}{3}}{H_0}\right). \tag{19}$$

But the result in (19) is different from that obtained in (15) and it is therefore concluded that the *B-B* formulation is not suitable for application here.

Landau-Lifshitz Case

The equation of motion is given in (7). With the same assumptions as earlier,we obtain, for the external tensor susceptibility components for a saturated ferrimagnetic sample of arbitrary shape but finite size,

$$\chi_1=\frac{\omega_m[\omega_0+\omega_m(N_y-N_z)+j\omega\alpha]+\alpha^2\omega_m[\omega_0+\omega_m(N_y-N_z)]}{[\omega_0+\omega_m(N_x-N_z)+j\omega\alpha][\omega_0+\omega_m(N_y-N_z)+j\omega\alpha]-\omega^2+\alpha^2\{\omega^2+[\omega_0+\omega_m(N_x-N_z)][\omega_0+\omega_m(N_y-N_z)]\}}, \tag{20}$$

$$\chi_2=\frac{\omega_m[\omega_0+\omega_m(N_x-N_z)+j\omega\alpha]+\alpha^2\omega_m[\omega_0+\omega(N_x-N_z)]}{[\omega_0+\omega_m(N_x-N_z)+j\omega\alpha][\omega_0+\omega_m(N_y-N_z)+j\omega\alpha]-\omega^2+\alpha^2\{\omega^2+[\omega_0+\omega_m(N_x-N_z)][\omega_0+\omega_m(N_y-N_z)]\}}, \tag{21}$$

$$\mathcal{K}=\frac{\omega_m\omega}{[\omega_0+\omega_m(N_x-N_z)+j\omega\alpha][\omega_0+\omega_m(N_y-N_z)+j\omega\alpha]-\omega^2+\alpha^2\{\omega^2+[\omega_0+\omega_m(N_x-N_z)][\omega_0+\omega_m(N_y-N_z)]\}}. \tag{22}$$

These can easily be simplified; for a spherical shape with $N_j=\frac{1}{3}$, we have

$$\chi_1=\chi_2=\frac{\omega_m\omega_0}{\omega_0^2-\omega^2+2j\omega\omega_0\alpha} \tag{23}$$

[13] N. Bloembergen, "Magnetic resonance in ferrites," Proc. IRE, vol. 44, pp. 1259–1269; October, 1956.

[14] H. Callen, "A ferromagnetic dynamical equation," *J. Phys. Chem. Solids*, vol. 4, no. 4, pp. 256–270; 1958.

and

$$\mathcal{K} = \frac{\omega_m \omega}{\omega_0^2 - \omega^2 + 2j\omega\omega_0\alpha} \cdot \tag{24}$$

Again, with $\alpha = \gamma\Delta H_0/2\omega_0$, the resonance behavior of external susceptibility gives

$$Q_u\Big|_{\text{sphere, } L\text{-}L \text{ formulation}} = \frac{H_0}{\Delta H_0} \cdot \tag{25}$$

This agrees with Q_u obtained for a sphere in (15) from the basic derivation. Thus, for samples of spherical shape, it is concluded that, of the two phenomenological damping mechanisms, the Landau-Lifshitz formulation is more appropriate than the Bloch-Bloembergen formulation. Hence, in the derivation of the equivalent circuit for YIG coupling, when the RF magnetic fields are elliptically polarized, the external tensor susceptibility components derived with the Landau-Lifshitz formulation will be used.

Analysis of Coupling

One way of analyzing the transmission characteristics of a resonance transmission filter is to reduce it to an equivalent circuit and then to compare the transmission characteristics with those of an RLC resonance filter. The approach that will be followed here is to obtain the open-circuit impedance parameters for the ferrite resonator coupling mechanism between two circuits when the RF magnetic fields due to these circuits are elliptically polarized. These are then compared with the open-circuit impedance parameters of a lumped-constant RLC resonance transmission filter to obtain the corresponding quantities, and then the application of filter-circuit theory gives the desired quantities which describe the coupling. This procedure has been applied to the ferrimagnetic resonance filter for the restricted case for which the RF magnetic field is linearly polarized by Carter.[3] The derivation in this paper is based upon Carter's work and extends the technique to the case for which the RF magnetic fields are elliptically polarized. This is done by considering two separate linearly polarized RF magnetic fields in time and space quadrature, making up the given elliptically polarized RF magnetic fields. The two components of the fields are considered to constitute two separate systems which have the corresponding fields of the two circuits at right angles, and the two systems are themselves in quadrature. Each of these systems gives rise to voltages, in accordance with the results from Carter's derivation for linearly polarized RF magnetic fields, which are in time quadrature. Hence, the total voltage induced is the vector sum of the two components. These voltages are related to the total longitudinal currents in the two circuits, from which the open-circuit impedance parameters are inferred.

Consider two RF circuits at right angles to each other, and such that at the location of the YIG sphere the RF magnetic fields due to both the circuits are elliptically polarized. Fig. 1 shows the coordinate system in the analysis. The coordinate system for circuit 1 is x_1, y_1, z_1, with y_1 being the direction of wave propagation; the coordinate system for circuit 2 is x_2, y_2, z_2, with y_2 being the direction of wave propagation; the directions y_1 and y_2 are at right angles. The coordinate axes for the YIG coupling sphere are x, y and z. The axes z, z_1, z_2 coincide. The dc magnetic field is applied along the z axis.

The following assumptions have been made:

1) That the YIG sphere is resonant at the uniform precession mode.
2) That the sphere size is small compared to free-space wavelength, so that the RF magnetic fields due to both the circuits can be assumed to be uniform over the entire sphere.
3) That the circuits propagate only the dominant mode.
4) That the circuits are lossless and there is no coupling between the two circuits in absence of the YIG coupling sphere.

The subscripts 1 and 2 will denote various quantities as applied to circuits 1 and 2, respectively. Let the RF magnetic field at the YIG sphere due to circuit 1 be h_{RF_1} for a wave traveling in the $+y_1$ direction, and the RF magnetic field for the *YIG* sphere due to circuit 2 be h_{RF_2} for a wave traveling in the $+y_2$ direction.

For elliptically polarized RF magnetic fields,

$$h_{\text{RF}_1} = \hat{a}_{x_1} h_{x_1} + j\hat{a}_{y_1} h_{y_1} \tag{26}$$

and

$$h_{\text{RF}_2} = \hat{a}_{x_2} h_{x_2} + j\hat{a}_{y_2} h_{y_2} \tag{27}$$

where $\hat{a}$'s are unit vectors in given directions. Hence, the RF magnetization in the YIG sphere can be given as

$$\boldsymbol{m} = \chi_{\text{ext}} \cdot \boldsymbol{h}_{\text{RF}} \tag{28}$$

where components of external tensor susceptibility for a sphere are obtained in (23) and (24). As remarked earlier, the magnetizations m_x and m_y will be broken up into two components each, each one arising from the corresponding linearly polarized components of h_{RF} in either one of the circuits, *viz.*, h_{x_1} and h_{x_2}, and h_{y1} and h_{y_2}, these two systems being in time quadrature.

Omitting lengthy derivation, the open-circuit impedance parameters for the coupling through a YIG sphere, when the RF magnetic fields are elliptically polarized, are

$$Z_{11} = j\omega\omega_m\mu\vartheta \frac{(\omega_0 k_{x_1}^2 + \omega k_{y_1}^2)}{\left(\omega_0^2 - \omega^2 + j\dfrac{\omega\omega_0}{Q_u}\right)}, \tag{29}$$

$$Z_{12} = \omega\omega_m\mu\vartheta \frac{(\omega k_{x_1}k_{x_2} + \omega_0 k_{y_1}k_{y_2})}{\left(\omega_0^2 - \omega^2 + j\frac{\omega\omega_0}{Q_u}\right)}, \tag{30}$$

$$Z_{21} = -\omega\omega_m\mu\vartheta \frac{(\omega k_{x_1}k_{x_2} + \omega_0 k_{y_1}k_{y_2})}{\left(\omega_0^2 - \omega^2 + j\frac{\omega\omega_0}{Q_u}\right)}, \tag{31}$$

$$Z_{22} = j\omega\omega_m\mu\vartheta \frac{(\omega_0 k_{x_2}^2 + \omega k_{y_2}^2)}{\left(\omega_0^2 - \omega^2 + j\frac{\omega\omega_0}{Q_u}\right)}, \tag{32}$$

where

$$k_{x_1} = \frac{h_{x_1}}{I_1},$$

$$k_{x_2} = \frac{h_{x_2}}{I_2},$$

$$k_{y_1} = \frac{h_{y_1}}{I_1},$$

$$k_{y_2} = \frac{h_{y_2}}{I_2},$$

and

I_1 = Total longitudinal current in circuit 1
I_2 = Total longitudinal current in circuit 2
ϑ = Volume of the YIG sample.

Comparing the open-circuit impedance parameters in (29)–(32) with those for an RLC resonance transmission filter, it is seen that the equivalent curcuit for the YIG coupling between two circuits, when the RF magnetic fields are elliptically polarized, is as shown in Fig. 2.

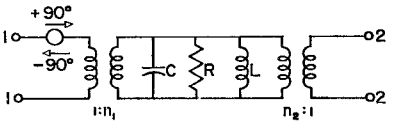

Fig. 2—Equivalent circuit for coupling through a YIG sphere when the RF magnetic fields are elliptically polarized. The open-circuit impedance parameters are given in (29),-(32).

With matched input and ouput,

$$Q_{e_1} = \frac{Z_{0_1}}{\omega_m\mu\vartheta(k_{x_1}^2 + k_{y_1}^2)}, \tag{33}$$

$$Q_{e_2} = \frac{Z_{0_2}}{\omega_m\mu\vartheta(k_{x_2}^2 + k_{y_2}^2)}. \tag{34}$$

where

Z_0 = Characteristic impedance of the RF circuit.

Input coupling parameter

$$\beta_1 = \frac{Q_u}{Q_{e_1}}. \tag{35}$$

Output coupling parameter

$$\beta_2 = \frac{Q_u}{Q_{e_2}}. \tag{36}$$

Transmission through such a coupling mechanism, between terminals 1-1 and 2-2 of the equivalent circuit, is given as

$$T(\omega_0) = \frac{4\beta_1\beta_2}{(1 + \beta_1 + \beta_2)^2} \tag{37}$$

and

$$Q_L = \frac{Q_u}{1 + \beta_1 + \beta_2} \tag{38}$$

where Q_L is the over-all Q of the filter.

Eqs. (37) and (38) describe the behavior of the coupling mechanism analyzed, but do not give the relative amplitudes of the two waves in the two arms of the secondary circuit, nor do they give the amount of energy coupled into terminals 1-1 from the primary circuit when the energy is traveling in the two different directions in the primary circuit. This is due to the fact that the magnetization in the YIG sphere is precessing in the positive direction (in relation to the dc magnetic field) and only the positively circularly polarized component of the RF magnetic field is coupled to the magnetization, *i.e.*, coupled into terminals 1-1.

It is relatively easy to obtain the transmission coefficient between various ports, assuming negligible loss in YIG sphere, *i.e.*, high Q_u. Only the results will be stated here.

The behavior of the four-port circuit can be expressed in the form of a scattering matrix. Fig. 1 shows the port nomenclature also. The phase information is omitted from the elements of the scattering matrix, as it is unimportant as long as one is concerned with insertion loss between two given ports.

$$\begin{pmatrix} R_1 \\ R_2 \\ R_3 \\ R_4 \end{pmatrix} = \begin{pmatrix} S_{11} & S_{12} & S_{13} & S_{14} \\ S_{21} & S_{22} & S_{23} & S_{24} \\ S_{31} & S_{32} & S_{33} & S_{34} \\ S_{41} & S_{42} & S_{43} & S_{44} \end{pmatrix} \begin{pmatrix} H_1 \\ H_2 \\ H_3 \\ H_4 \end{pmatrix} \tag{39}$$

where

R_m = Amplitude of wave going out of port m
H_m = Amplitude of wave incident at port m.

Scattering-matrix elements are given for the case of a high-Q_u YIG sphere (*i.e.*, neglibible loss in the YIG sphere) as

$$S_{11} = (T)^{1/2}AB$$
$$S_{12} = (T)^{1/2}BD$$
$$S_{13} = [(1 - TB^2) - TA^2B^2]^{1/2}$$
$$S_{14} = (T)^{1/2}BC$$
$$S_{21} = (T)^{1/2}AC$$
$$S_{22} = (T)^{1/2}CD$$
$$S_{23} = (T)^{1/2}BC$$
$$S_{24} = [(1 - TC^2) - TC^2D^2]^{1/2}$$
$$S_{31} = [(1 - TA^2) - TA^2B^2]^{1/2}$$
$$S_{32} = (T)^{1/2}AD$$
$$S_{33} = (T)^{1/2}AB$$
$$S_{34} = (T)^{1/2}AC$$
$$S_{41} = (T)^{1/2}AD$$
$$S_{42} = [(1 - TD^2) - TC^2D^2]^{1/2}$$
$$S_{43} = (T)^{1/2}BD$$
$$S_{44} = (T)^{1/2}CD.$$

It can be seen that the junction is now lossless, due to the assumption of negligible loss in the YIG sphere. Here

$$A^2 = \frac{1}{1 + \left(\frac{k_{x_1} + k_{y_1}}{k_{x_1} - k_{y_1}}\right)^2} \qquad B^2 = \frac{1}{1 + \left(\frac{k_{x_1} - k_{y_1}}{k_{x_1} + k_{y_1}}\right)^2}$$

$$C^2 = \frac{1}{1 + \left(\frac{k_{x_2} + k_{y_2}}{k_{x_2} - k_{y_2}}\right)^2} \qquad D^2 = \frac{1}{1 + \left(\frac{k_{x_2} - k_{y_2}}{k_{x_2} + k_{y_2}}\right)^2}$$

When the dc magnetic field is reversed, A^2 and B^2 are interchanged, and C^2 and D^2 are interchanged.

$T(\omega_0)$ is defined in (37).

Examining the elements of the scattering matrix, it can be seen that the device is nonreciprocal and that the nonreciprocal behavior is optimum when the RF magnetic fields are circularly polarized. In this case there is no reflected wave at the input port, and in this respect a ferrimagnetic filter gives the same results as a transmission filter using a circularly polarized cavity.[15,16] The nonreciprocal behavior deteriorates as the ellipticity of the RF magnetic field is increased. Finally, for the case for which the RF magnetic fields are linearly polarized, this circuit becomes reciprocal.

Regarding the arbitrariness involved in the results of (29)–(32), due to arbitrary definition of Z_0 for a circuit, it can be said that the results in the above equations will not depend upon the arbitrariness of the definition of Z_0 as long as that definition is consistent with the definition of the voltage and current in the equivalent-circuit representation of the YIG coupling mechanism. It is perfectly possible to define Z_0 in any desired manner, as long as the derivation of the open-circuit impedance parameter for the YIG coupling is modified accordingly.

[15] W. L. Whirry and C. E. Nelson, "Ferrite loaded, circularly polarized microwave cavity filters," IRE TRANS. ON MICROWAVE THEORY AND TECHNIQUES, vol. MTT-6, pp. 59–66; January, 1958.

[16] C. E. Nelson, "Circularly polarized microwave cavity filters," IRE TRANS. ON MICROWAVE THEORY AND TECHNIQUES, vol. MTT-5, pp. 136–147; April, 1957.

Experimental Devices and Measurements

To obtain circularly or, in general, elliptically polarized RF magnetic fields for the coupling transmission lines at X-band frequencies, it is seen that waveguides are most suitable, due to low loss in the transmission. With rectangular waveguides operating in TE_{10} modes, off axis and away from sidewalls, the RF magnetic fields are elliptically polarized but the ellipticity is frequency dependent.

For a wave traveling in $+y$ direction,

$$k_x = \frac{h_x}{I} = \frac{\pi}{2a} \sin \frac{\pi x}{a}, \tag{40}$$

$$k_y = \frac{h_y}{I} = -\frac{\pi}{2a}\left(\frac{\lambda_0}{2a}\right) \frac{1}{\sqrt{1 - \left(\frac{\lambda_0}{2a}\right)^2}} \cos \frac{\pi x}{a} \tag{41}$$

where

a = width of the rectangular waveguide
x = off-axis distance of location of YIG sphere
λ_0 = free space wavelength.

$|k_x|$ and $|k_y|$ have been shown in Fig. 3 as functions of frequency for an X-band waveguide with various locations X. This shows how the ellipticity of an RF magnetic field varies with frequency in a rectangular waveguide. Also $|k_x| = |k_y|$ are points for circular polarization.

The experimental filter consisted of two rectangular waveguides at right angles with their broad faces in contact. In the common wall between the two guides, an aperture contains the YIG coupling sphere mounted on a dielectric rod at the end of a screw—to be inserted through a tapped hole directly across from the aperture. This arrangement allows the YIG sphere to be symmetrically located in the aperture with respect to the common wall and to line up the hard axis along the dc magnetic field. The waveguide heights were reduced to $\frac{1}{4}$ standard height using suitable tapers. Fig. 4 shows a photograph of the filter structure with the screw-in position.

Three different filter structures with different locations of the YIG sphere yield different characteristics. The forward and the reverse insertion losses for these filters are shown in Figs. 5–7, along with the theoretically computed results as expressed in the scattering matrix. The YIG sphere used in all these cases had a diameter of 0.060 in and a linewidth of 0.44 oersted. The theoretical results shown include a small (<1 db) addi-

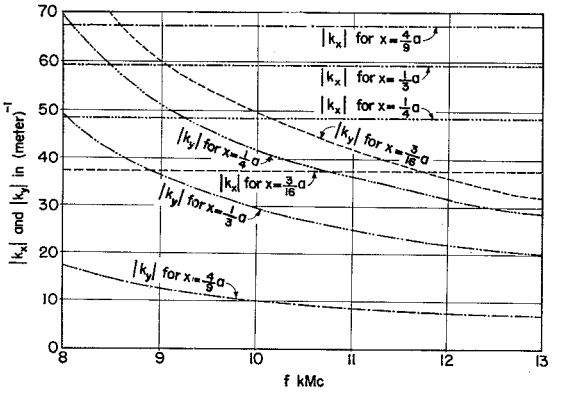

Fig. 3—$|k_x|$ and $|k_y|$, as defined in (40) and (41), shown as functions of frequency for an X-band waveguide for various x. Frequency, for which $|k_x| = |k_y|$ for a particular x corresponds to circular polarized RF magnetic field.

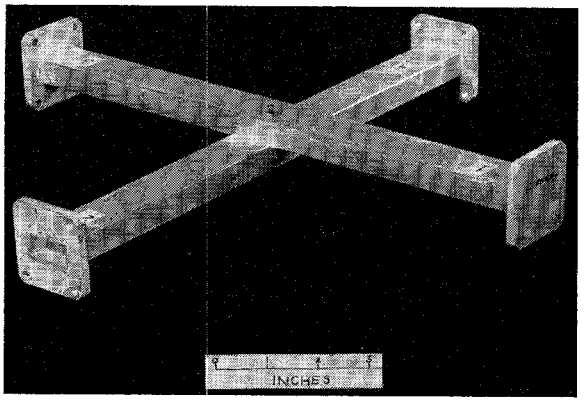

Fig. 4—Photograph of the filter structure experimentally investigated. The screw, which holds the YIG sphere in position between the two waveguides, is also visible.

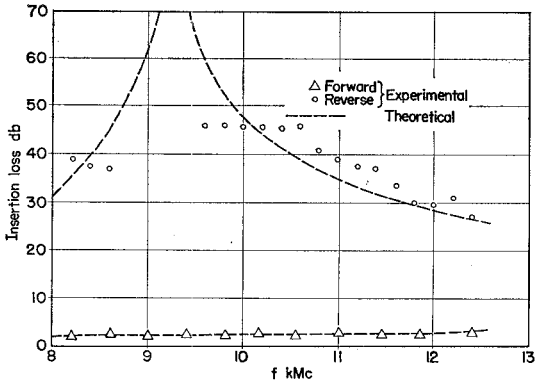

Fig. 5—Forward and reverse insertion loss between ports 2 and 1 (see Fig. 1) as functions of frequency for the filter with $x=\frac{1}{4}a$. The dc magnetic field is adjusted to resonate the sphere at the frequency of measurement. All the four ports are terminated with matched loads. Theoretical results are also shown for comparison. (YIG sphere, diameter=0.060 in, $\Delta H_0=0.44$ oersted.)

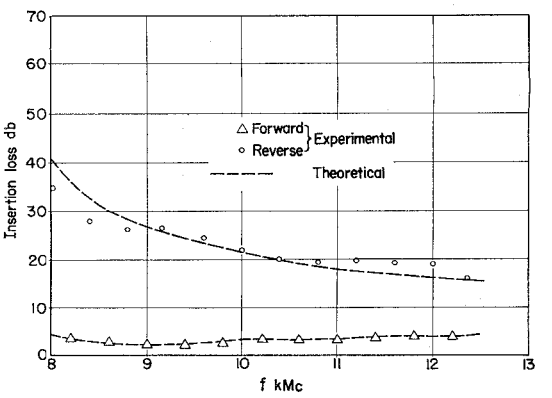

Fig. 6—Forward and reverse insertion loss between ports 2 and 1 (see Fig. 1) as functions of frequency for the filter with $x=\frac{1}{3}a$. The dc magnetic field is adjusted to resonate the YIG sphere at the frequency of measurement. All the four ports are terminated with matched loads. Theoretical results are also shown for comparison. (YIG sphere diameter=0.060 in, $\Delta H_0=0.44$ oersted.)

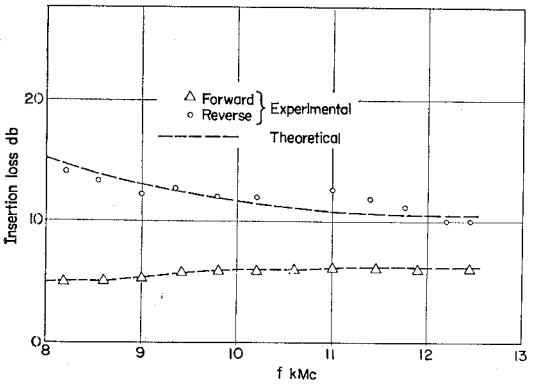

Fig. 7—Forward and reverse insertion loss between ports 2 and 1 (see Fig. 1) as functions of frequency for the filter with $x=\frac{4}{9}a$. The dc magnetic field is adjusted to resonate the YIG sphere at the frequency of measurement. All the four ports are terminated with matched loads. Theoretical results are also shown for comparison. (YIG sphere diameter=0.060 in, $\Delta H_0=0.44$ oersted.)

tional loss, due to the losses in the waveguide configuration. The volume and the linewidth of the YIG sphere are important parameters in determining the insertion loss of the filter as seen from (33)–(38). Due to the very small size of the YIG sphere, the dielectric constant of 8–10 of the YIG has neglibible effect on the insertion loss and hence this has been neglected.

The total Q, or the Q_L, of these three filters can be calculated with the help of (38) and Fig. 3, taking into account the reduction in effective volume due to the fact that the YIG sphere is not wholly located in either one of the guides. The experimental results are shown in Fig. 8 for the three cases. This shows a very interesting property of using elliptically polarized RF magnetic fields for coupling through the YIG sphere in a rectangular waveguide. The Q_L for $(x=1/4a)$ filter increases as frequency is increased, and the bandwidth remains substantially constant over the entire frequency range from 8.2 to 12.4 kMc. The Q_L for $(x=3/16a)$ filter is essentially constant over the X band, for the $(x=4/9a)$ filter Q_L decreases as frequency is increased.

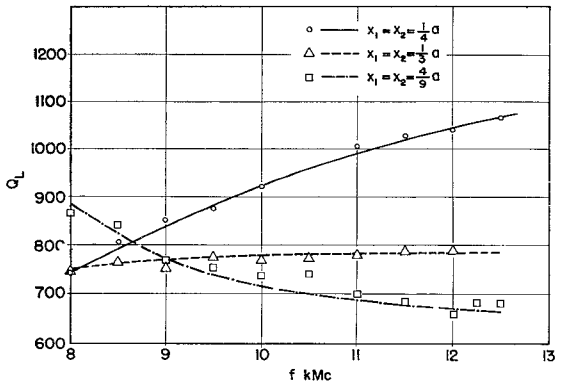

Fig. 8—Q_L or the total loaded Q of the filter as functions of frequency for three filters with different x. The Q_L is measured by tuning the dc magnetic field to resonate the YIG sphere at the frequency of measurement and then determining the transmission 3-db bandwidth by changing the frequency on either side of the resonance frequency. All the four ports of the filters are terminated with matched loads. (YIG sphere diameter=0.060 in, $\Delta H_0=0.44$ oersted.)

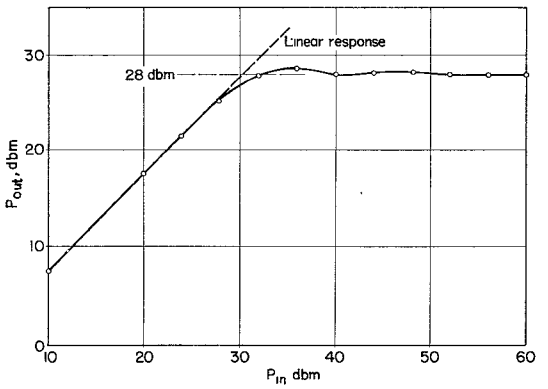

Fig. 9—Steady-state signal limiting behavior measured on $x=\frac{1}{4}a$ filter. The output power level is seen to be limited at +28 dbm for all higher input power levels. (YIG sphere diameter=0.060 in, $\Delta H_0=0.44$ oersted.)

The saturation of RF magnetization causes the amplitude of the RF magnetization to be limited at a certain level when the power is increased beyond the critical power level.[17–19] Beyond this power level, the resonance susceptibility drops and there is a decrease in the coupling through the YIG sphere. Due to this increase in insertion loss, the filter acts as a narrow-band transmission limiter for high-power levels. The critical power level depends upon the ellipticity of RF magnetic field as seen from theory.[17–19] Thus, the limiting power level is the minimum for circularly polarized RF magnetic fields and the maximum for the linearly polarized case. The steady-state limiting behavior of the filter with $(x=1/4a)$ is shown in Fig. 9 with $f=9.3$ kMc, which corresponds to the case of circularly polarized RF magnetic field at the YIG sphere in the waveguide.

For input pulses with power level higher than the limiting power level, the output pulse from the filter shows the typical leakage spike at the leading edge. Measurements on the duration and amplitude of the leakage spike and the leakage energy in the spike, as functions of input pulse power level, have been shown in Fig. 10. From Fig. 10 it can be seen that leakage energy in the spike is greater than that required to burn out a 1N26 detector crystal.

The unloaded Q_u of the polished YIG sphere, measured as a function of frequency, is shown in Fig. 11. It can be inferred from this that the linewidth in single-crystal YIG remains constant as frequency is changed, and that Q_u increases linearly with frequency. These measurements were made with the dc magnetic field

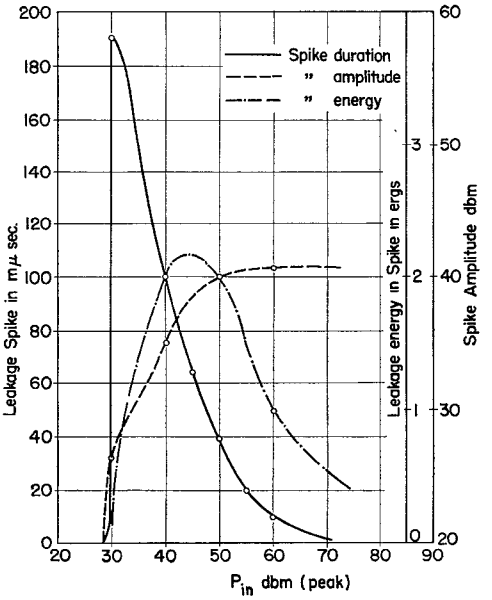

Fig. 10—Transient signal limiting behavior of $x=\frac{1}{4}a$ filter, showing the duration, amplitude and energy of leakage spike at the leading edge of the output pulse as functions of input power (peak). The input pulse has a constant rise time of 10 mμ sec. (YIG sphere diameter=0.060 in, $\Delta H_0=0.44$ oersted.)

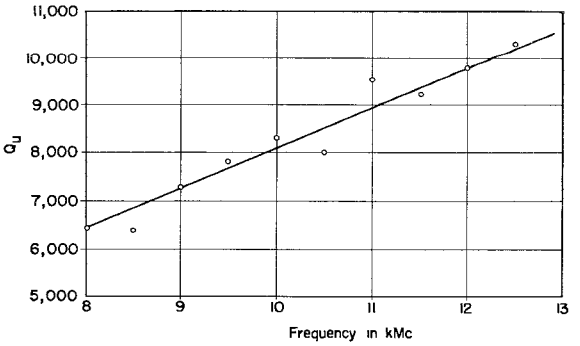

Fig. 11—Unloaded Q of a polished sphere of single crystal YIG measured as function of frequency. The measurement at each frequency was carried out with $Q_e \gg Q_u$, *i.e.*, very light coupling. (Sphere diameter=0.060 in.)

[17] E. Schlömann, "Ferromagnetic Resonance at High Power Levels," Raytheon Co., Waltham, Mass. Rept. No. R-48; October 1, 1959.

[18] H. Suhl, "Nonlinear behavior of ferrites at microwave high signal levels," PROC. IRE, vol. 44, pp. 1270–1284; October, 1956.

[19] H. Suhl, "Note on saturation of main resonance in ferromagnetics," *J. Appl. Phys.*, vol. 30, pp. 1961–1964; December, 1959.

along the hard axis of the single crystal from which the sphere is ground, and it seems to give the largest Q_u. The results reported here are in contrast with those reported by Carter[4] wherein measured Q_u is reported to be dropping as frequency is increased beyond 8 kMc, and the results reported here are believed to be correct.

Conclusion

The particular application of the analysis has shown agreement between the theory and the experiment. However, it may not be thought that only waveguides can be used to obtain a nonreciprocal filter using a YIG resonator. At lower frequencies, at which waveguide size becomes an important aspect of the problem, a coaxial line, with half of it loaded with a dielectric, can be used to obtain a circularly polarized RF magnetic field. However, as mentioned in the section on the unloaded Q_u, there is a lower frequency limit for the usefulness of spherical samples of ferrimagnetic material. Also, it is shown that a cylindrical sample shows a larger Q_u at lower frequencies, but it cannot possibly resonate at frequencies lower than $\omega_m/2$. Thus the only solution is in using a material with lower saturation magnetization, but, as seen from (33) and (34), this causes a higher Q_e which results into a higher insertion loss in the pass band. Thus, in order to keep the coupling parameter β constant and as high as possible, for lowering the lower limit on frequency limitation, a ferrimagnetic material with lower M_s and a correspondingly smaller linewidth will be necessary, *i.e.*, keep $M_s/\Delta H_0$ or Q_u/Q_e constant.

Acknowledgment

The author would like to express his thanks to Prof. Dean A. Watkins for suggesting the topic and for his continued interest and encouragement in the work, and to Prof. A. E. Siegman for many helpful discussions.

Propagation on Modulated Corrugated Rods*

C. C. WANG†, senior member, ire, and E. T. KORNHAUSER‡, senior member, ire

Summary—**The velocity of surface-wave propagation on two types of axially modulated corrugated rods has been measured experimentally. Type A has a constant outer diameter and sinusoidally varying slot depth, while in type B the slot depth varies in virtue of a modulated outer diameter. In both cases the measured phase velocity is about ten per cent less than that for a uniformly corrugated rod with the average slot depth and outer diameter, but agrees within two per cent over the frequency range used with the value calculated from an analysis based on the Mathieu equation.**

I. Introduction

Interest in the properties of modulated surface-wave structures stems from their application as end-fire antennas.[1] Further work has indicated the possibility of producing radiation in other desired directions,[2] and most recently a technique has been presented for designing the modulations of a plane corrugated surface so as to support several slow waves simultaneously.[3]

The analysis of the radiation characteristics of finite lengths of such structures has been based on the surface-wave propagation properties of the infinitely long structure. To that end experiments were performed on two types of corrugated cylinders, which are the most useful configuration for practical application, and their surface-wave phase velocity measured as a function of frequency. The infinitely long structure was simulated by the use of parallel reflecting planes at each end.

Structure A, shown in Fig. 1, is a cylinder with constant outer diameter of 0.85 in, whose inner diameter (at the bottom of the slots) varies sinusoidally in the axial direction between 0.4 in and 0.85 in. The average inner diameter is thus 0.625 in and the average slot depth 0.1125 in. The width of each slot is 0.05 in, and their spacing is 0.1 in. The structure was constructed by stacking brass washers of 0.05 in thickness and various diameters on a steel rod 0.2 in in diameter with sufficient axial pressure to insure good electrical contact between washers. The axial period of the modulation is 1.2 in, and the whole structure is about 11 in long.

* Received by the PGMTT, November 27, 1961. This work is part of a thesis submited by C. C. Wang to Brown University in fulfillment of the M.S. degree and was supported by the Air Force Cambridge Research Laboratory under Contract AF19(604)-4561.

† Communications Systems Research Section, Jet Propulsion Laboratory, California Institute of Technology, Pasadena, Calif.

‡ Brown University, Providence, R. I.

[1] J. C. Simon and V. Biggi, "Un nouveau type d'aérien et son application à la transmission de télévision à grande distance," *L'Onde Elec.*, vol. 34, pp. 883–891; November, 1954.

[2] A. S. Thomas and F. J. Zucker, "Radiation from modulated surface wave structures I," 1957 IRE National Convention Record, pt. 1, p. 153–160; also R. L. Pease, "Radiation from modulated surface-wave structures," *ibid.*, pp. 161–165.

[3] J. T. Bolljahn, "Synthesis of modulated corrugated surface-wave structures," IRE Trans. on Antennas and Propagation, vol. AP-9, pp. 236–241; May, 1961.